Hindawi
International Journal of Antennas and Propagation
Volume 2023, Article ID 9918890, 10 pages
https://doi.org/10.1155/2023/9918890

*Research Article*

# Quantitative Study of Load Stability of Quadrotor Based on Lyapunov Exponents

**Tiantian Dong,[1,2] Yonghong Zhang ,[1] Yunping Liu,[1] and Cheng Chen[1]**

[1]*Nanjing University of Information Science and Technology, School of Electronics and Information Engineering, Nanjing 210044, China*
[2]*Jiangsu Vocational College of Information Technology, Wuxi 214153, China*

Correspondence should be addressed to Yonghong Zhang; zyh@nuist.edu.cn

Received 6 December 2022; Revised 17 March 2023; Accepted 4 April 2023; Published 19 April 2023

Academic Editor: Mauro Parise



This paper addresses the issue of dynamic instability in quadrotor caused by changes in load mass during flight. To tackle this problem, the Lyapunov exponent method is adopted to study the dynamics and motion stability of the system. This approach resolves the challenge of constructing system eigenvalues due to the nonlinearity and high order of the quadrotor. To enhance the reliability of stability analysis, a quantitative relationship between system dynamics parameters and motion stability is established by combining the dynamic model with the Lyapunov exponent method. This approach compensates for inaccuracies in theoretical modeling analysis caused by factors such as load mass changes. The experiments demonstrate that changing the wheelbase and load mass improves flight motion stability, ensuring the reliability of the quadrotor flight system. Overall, this paper provides an in-depth analysis of the motion stability of a quadrotor and proposes a reliable method for stability analysis that accounts for changes in load mass during flight.

## 1. Introduction

The operating area of the quadrotor is primarily located in the near-ground space with complex terrain and frequent airflows, particularly in the fields of emergency response, atmospheric exploration, and cargo transportation, making the motion stability of the entire quadrotor system particularly important [1–4]. In general, quadrotors are required to perform tasks such as hanging or releasing payloads, and changes in structural parameters can alter the dynamic characteristics and motion stability of the entire quadrotor system, leading to dynamic instability problems such as pendulum oscillation, decreased accuracy, and uncontrolled crashes [5–7].

The motion stability of the quadrotor during payload release is essentially a problem of motion stability under variable structural parameters. Motion stability refers to the property of a system to return to its motion state after being deviated from that state by external disturbances [8]. For unstable systems, the effects of disturbances are significant, such that even small disturbance forces can cause large deviations from the intended motion over time, resulting in oscillations, swaying, and loss of control. Amiri et al. used the Newton-Euler formula to establish a dynamic model of a vertical takeoff and landing (VTOL) quadrotor with lateral and longitudinal rotor tilting mechanisms to improve the pitch, yaw, and roll stability of the system. However, it is inevitable that structural parameter changes and atmospheric disturbances will occur during quadrotor payload release, which requires the entire system to be designed with high robust stability [9]. Therefore, establishing a quantitative relationship between quadrotor structural parameter changes and their motion stability is of significant engineering and practical significance for guiding mechanical design and optimizing control systems to improve motion stability. Liu and Amiri et al. used the concept of Lyapunov indices to improve system reliability and stability from the perspective of structural parameter design [10, 11].

Furthermore, during the payload delivery process of the quadrotor, changes in parameters and uncertain aerodynamic loads can turn the entire system into a complex,

high-order, strongly coupled, nonlinear system [12, 13]. However, when traditional direct solving of dynamic equations or the Lyapunov direct method is used for analysis, there are often problems of complex equations difficult to solve and Lyapunov function difficult to construct [14], and it is difficult to give a quantitative relationship between structural parameter changes and system motion stability. Therefore, how to quantitatively analyze the motion stability of a quadrotor during payload delivery has become one of the urgent scientific issues to be solved currently [15–19].

Due to the ability of Lyapunov exponents to quantitatively describe the degree of divergence or convergence between two trajectories, one perturbed and one unperturbed, over time, this can be used as a method for quantitatively analyzing the motion stability of the quadrotor systems during payload delivery. Compared to direct Lyapunov methods, the main advantage of the approach presented in this paper is the ability to quantitatively describe the relationship between dynamic parameter changes and system motion stability, providing reference design criteria for improving stability and reducing control energy consumption [20–24]. Through comparative experiments, this paper demonstrates that changes in the system's mechanical design and mass parameters, specifically the wheelbase and payload mass, can improve flight stability.

## 2. Analysis of System Stability Based on Lyapunov Exponents

The Lyapunov exponent describes the average exponential rate at which the trajectories of a system's disturbed initial value and original initial value converge or diverge over time. When the Lyapunov exponent is less than 0, the phase trajectories of the system converge to a stable fixed point, and the entire system is stable. When the Lyapunov exponent is greater than 0, the system is unstable or chaotic. When the Lyapunov exponent is 0, the phase trajectories are periodic [25].

The Lyapunov exponent can be obtained by either the kinetic equation or the time series of the state quantity, and the calculation method based on the equation is used here, expression is as follows:

$$\lambda = \lim_{n \longrightarrow \infty} \frac{1}{n} \sum_{i=0}^{n-1} \ln \left| \frac{df(X)}{dX} \right|_{X_i}. \quad (1)$$

Equation of state (1) is obtained by the transformation of the dynamic equations of a nonlinear system. The size of the Lyapunov exponent is determined by the Jacobian matrix $|\mathrm{d}f/\mathrm{d}X|$ of function $f(X)$ at $X_i$, the whole calculation of which is as follows.

First, modular kinematics and equations based on operators are constructed, and their Euler–Poincare formula is as follows:

$$\dot{q} = V(q)p, \quad (2)$$

$$M(q)\dot{p} + C(q,p)p + F(p,q,u) = 0. \quad (3)$$

In equations (2) and (3), $q$ represents the generalized coordinate vector, and there exists a mapping relationship between $q$ and $X$, which is obtained by transforming the transfer function into a state equation. The dynamic equations are then converted into state equations as follows:

$$\frac{\mathrm{d}X(t)}{\mathrm{d}t} = f(X(t)). \quad (4)$$

Next, calculate the Jacobian matrix:

$$\left| \frac{\mathrm{d}f(X)}{\mathrm{d}X} \right|_{X_i}. \quad (5)$$

Finally, according to (4), the Jacobian can be calculated to get the Lyapunov index shown in (5).

## 3. System Modeling and Lyapunov Exponent Computation

Establish a quadrotor model, as shown in Figure 1, the quadrotor body coordinate $B(X_b, Y_b, Z_b)$ and the geodetic coordinate $E(X_e, Y_e, Z_e)$. The quadrotor is around a particle, found in the center of the structure, with mass $m$, the distance between the rotor and the center of the fuselage is $L$, and the thrust $U \in R$ is the vector sum of the 4 rotor lift is $F_n (n = 1, 2, 3, 4)$; $\phi$ is the roll angle of the around the $x$-axis;$\theta$ is the pitch angle of the around the $y$-axis; and $\psi$ is the yaw angle of the around the $z$-axis.

*3.1. Assumptions.* (1) The quadrotor is a rigid body and is completely uniformly symmetrical, (2) the origin $B$ of the body coordinates coincides completely with the center of mass of the unmanned aerial vehicle, and (3) the propellers of the quadrotor are rigid bodies, and their structure and elastic deformation are not considered.

Depending on the fuselage layout, drones can be divided into type "+" and type "×." This article adopts a "×" type, which has higher maneuverability than the "+" type. Newton's second law and Euler equation are used to show the model.

$$\dot{q} = V(q)p, \quad (6)$$

$$M(q)\dot{p} + C(q,p)p + F(p,q,u) = 0, \quad (7)$$

where $V(q)$ in (6) is the kinematic matrix and $M(q)$ and $C(q, p)$ in (7) are inertia matrix and gyroscope matrix, respectively, that can be as follows:

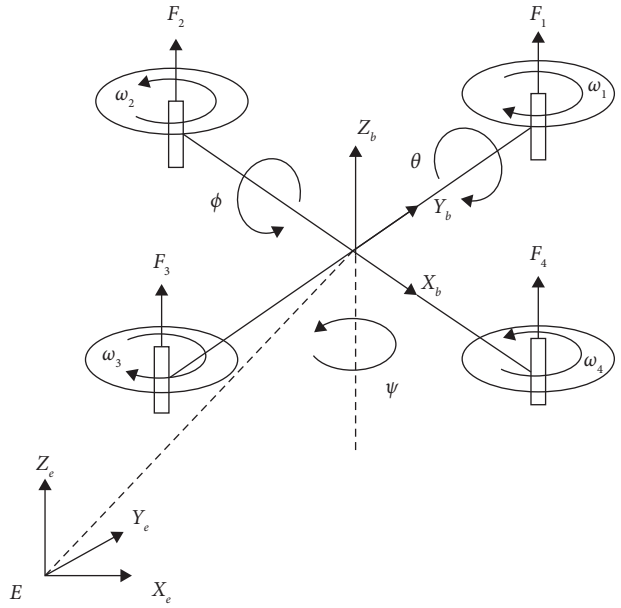


Figure 1: System diagram.

$$V(q) = \begin{bmatrix} 1 & 0 & 0 & 0\ 0\ 0 & \\ S_\phi T_\theta & C_\phi & S_\phi C_\theta^{-1} & 0\ 0\ 0 & \\ C_\phi T_\theta & -S_\phi & C_\phi C_\theta^{-1} & 0\ 0\ 0 & \\ 0\ 0\ 0 & & C_\theta C_\psi & C_\theta S_\psi & -S_\theta \\ 0\ 0\ 0 & & S_\phi S_\theta C_\psi - C_\phi S_\psi & S_\phi S_\theta S_\psi + C_\phi C_\psi & S_\phi C_\theta \\ 0\ 0\ 0 & & C_\phi S_\theta C_\psi + S_\phi S_\psi & C_\phi S_\theta S_\psi - S_\phi C_\psi & C_\phi C_\theta \end{bmatrix}, \tag{8}$$

$$M(q) = \begin{bmatrix} I_{X_b} & 0 & 0 & 0\ 0\ 0 & \\ 0 & I_{Y_b} & 0 & 0\ 0\ 0 & \\ 0 & 0 & I_{Z_b} & 0\ 0\ 0 & \\ 0\ 0\ 0 & & m & 0 & 0 \\ 0\ 0\ 0 & & 0 & m & 0 \\ 0\ 0\ 0 & & 0 & 0 & m \end{bmatrix}, \tag{9}$$

where $I_{X_b}, I_{Y_b}, and\ I_{Z_b}$ in (9) are the moment of inertia of the $X_b, Y_b,$ and $Z_b$ axes, respectively.

$$\begin{cases} U_1 = F_1 + F_2 + F_3 + F_4, \\ U_2 = F_2 + F_4, \\ U_3 = F_1 + F_3, \\ U_4 = K(F_1 + F_2 + F_3 + F_4). \end{cases} \tag{10}$$

In (10), $K = (C_Q/C_T)$, $C_Q$ is the rotor torque coefficient; Thrust $U_n(n = 1, \cdots, 4) \in R$ is the vector sum of four rotor thrust $F_n(\mathrm{n} = 1, \cdots, 4)$, $U_1$ is the vertical speed control quantity, $U_2$ is the roll input control quantity, $U_3$ is the pitch control input quantity, and $U_4$ is the yaw control quantity; $F$ is the pull force to each rotor.

$F(p, q, u)$ contains the sum of aerodynamic, gravity, and control inputs, which can be expressed as follows:

$$F(p, q, u) = \begin{bmatrix} -LU_2 \\ -LU_3 \\ -U_4 \\ mgS_\theta - U_1\left(C_\phi C_\psi S_\theta + S_\phi S_\psi\right) \\ -mgC_\theta S_\phi - U_1\left(-S_\phi C_\psi + C_\phi S_\theta S_\psi\right) \\ -mgC_\theta C_\phi - U_1 C_\phi C_\theta \end{bmatrix}, \tag{11}$$

where $S_\phi = \sin\phi$, $C_\phi = \cos\phi$, $S_\theta = \sin\theta$, $C_\theta = \cos\theta$, $C_\theta^{-1} = \sec\theta$, $T_\theta = \tan\theta$, $S_\psi = \sin\psi$, $C_\psi = \cos\psi$; and the g is the acceleration of gravity.

$$F = \frac{1}{2}\rho A C_T R^2 \Omega^2. \tag{12}$$

In (12), $A = \pi R^2$, $R$ is the radius of the rotor; $\rho$ is the air density, $C_T$ is the rotor lift coefficient, and $\Omega$ is the rotor speed.

$$p = (p, q, r, u, v, w)^T,$$
$$q = (\phi, \theta, \psi, X_b, Y_b, Z_b)^T. \quad (13)$$

Convert (4) and (5) into equations of state of the system:

$$\dot{X} = f(X). \quad (14)$$

Equation (14):

$$X = [q\ p]^T = (\phi, \theta, \psi, X_b, Y_b, Z_b, u, v, w)^T. \quad (15)$$

Based on the showed dynamic model, the Lyapunov exponent spectrum of the whole is obtained by combining (6) and (1). To calculate the Lyapunov exponent, take the time $T = 0.6$ and the number of iterations $K = 100$. Where the $T$ value is determined according to the sampling step, and the $K$ value is determined according to the empirical value. Given the first conditions, the vector is obtained by integral after the $K$ th iteration, and then GramSchm is orthogonalized and normalized. This process is repeated until the Lyapunov index reaches the maximum number of iterations $k$, and the resulting index $\lambda_1, \lambda_1 \cdots \lambda_6$ forms the Lyapunov exponent spectrum.

Based on the derivation process of equation (1), a quantitative relationship can be established between the main mechanical structural parameters of the quadrotor and the stability of the system during motion, as shown in Figure 2.

Figure 2: first, the equation is established, then the Jacobian matrix is calculated based on the equation, and finally the Lyapunov exponent is obtained. Where $V$ is kinematics matrix, $M$ is inertial matrix, $C$ is gyro matrix, and $F$ contains the sum of aerodynamic, gravity, and control inputs. According to the relationship between structural features and motion stability, the mass m of the system, the center distance L of the body, and the moment of inertia $I_{X_b}, I_{Y_b}, I_{Z_b}$ have influence on the Lyapunov exponent.

## 4. Simulation of Motion Stability

Quantitative analysis is of great significance in the field of multirotor quadrotor and is a theoretical prerequisite for studying motion stability. In this paper, based on the modeling of dynamic systems and the Lyapunov exponent method, load motion stability analysis based on hovering state is achieved, and on this basis, maximum load and hovering time are analyzed.

The following features are wanted for quadrotor dynamics modeling and estimation. The features in Table 1 are mainly obtained by direct measurement, empirical value estimation, and indirect experimental measurement. Among them, the features obtained by direct measurement are as follows: $m, g, L, R, \rho, n$, $C_b, R_b, U_b, K_b$, where the tensile force coefficient $C_T$ and the torque coefficient $C_Q$ are estimated by selecting the average

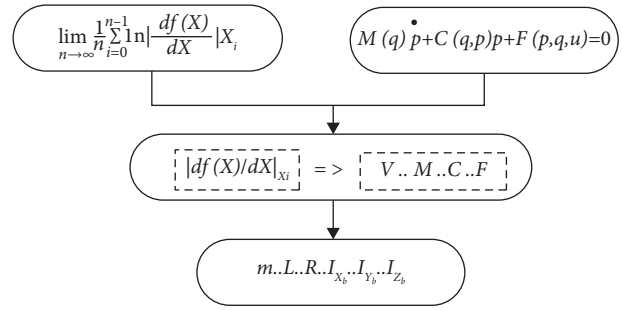


Figure 2: The relationship between structural features and stability.

Table 1: System structures feature table.

| Features | Symbolss | Numbers |
|---|---|---|
| System quality | $m$ | 1.527 kg |
| Acceleration | $g$ | 9.8 m/s$^2$ |
| Wheelbase | $L$ | 0.36 m |
| Tension coefficient | $C_T$ | $1.0792E-005$ N |
| Torque coefficient | $C_Q$ | $1.89E-007$ N.m |
| Rotor radius | $R$ | 0.12 m |
| Air density | $\rho$ | 1.293 kg/m$^3$ |
| Moment of inertia | $I_{X_b}$ | $9.5065E-003$ kg•m$^2$ |
| Moment of inertia | $I_{Y_b}$ | $1.00E-002$ kg m$^2$ |
| Moment of inertia | $I_{Z_b}$ | $1.658E-002$ kg•m$^2$ |
| Blade | $n$ | 4 |
| Battery capacity | $C_b$ | 5300 mAh |
| Battery resistance | $R_b$ | 0.01 Ω |
| Battery voltage | $U_b$ | 16.2 V |
| Max discharge rate | $K_b$ | 30C |
| Throttle command | $\sigma$ | 0.8 |

features with wide applicability through the experimental data of the two-blade propeller provided by the APC website. In summary, the total features of the quadrotor are shown in Table 1.

Among them, the main moment of inertia $I_{X_b}, I_{Y_b}$, and $I_{Z_b}$ is obtained by the double-line pendulum experiment. First, measure the moment of inertia of $X$ and $Y$ axes by the double-line pendulum experiment, then measure the moment of inertia of $Z$ axis by the four-line pendulum experiment, then consult the table of moment of inertia measurement features to decide the $\omega$ value and bring it into the moment of inertia calculation formula, and finally calculate the three-axis moment of inertia of the quadrotor.

*4.1. Optimization of Load Mass features.* The impact of the mass parameter $L$ on the attitude Lyapunov exponent of the quadrotor is shown in Figure 2. The Lyapunov exponent spectra of the system attitude are calculated separately when the load mass changes. CASE 1: When the quadrotor flies at an altitude of 10m and the load mass M = 0.56kg, the system is in position mode. CASE 2: When the quadrotor flies at an altitude of 10m and the load mass M = 1.02kg, the system is in position mode, as shown in Figure 3.

Figures 3 and 4: The variation of payload quality can improve the motion stability of the quadrotor. It can be concluded that when the quadrotor is in a stationary hovering state, the stability of the system in CASE 1 is better than that in CASE 2. In practical load flight processes, system stability can

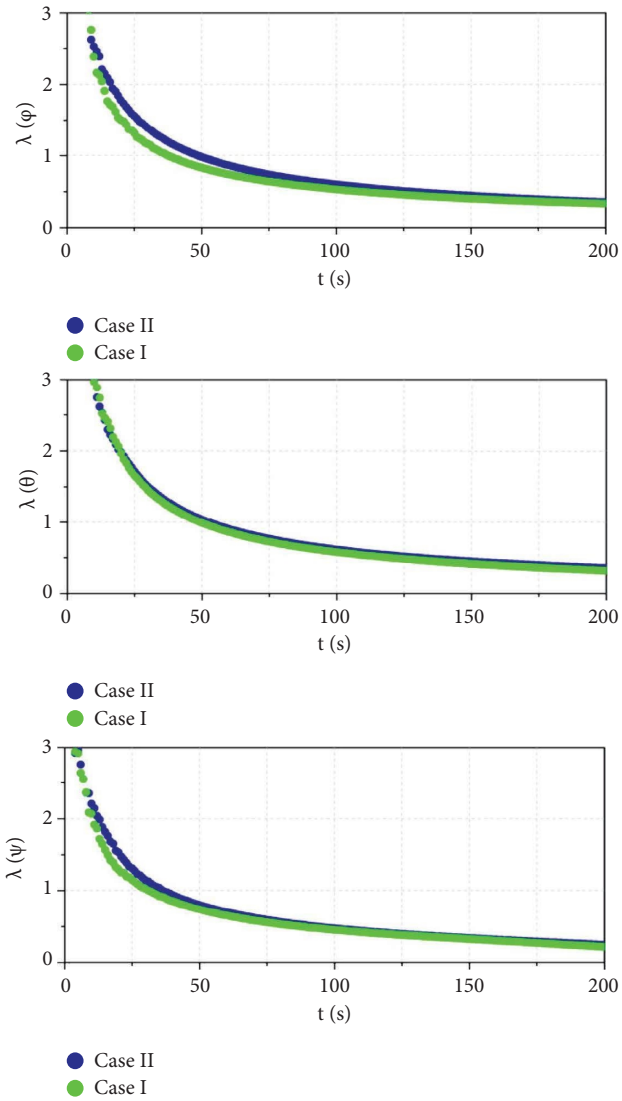


Figure 3: Lyapunov exponent spectrum.

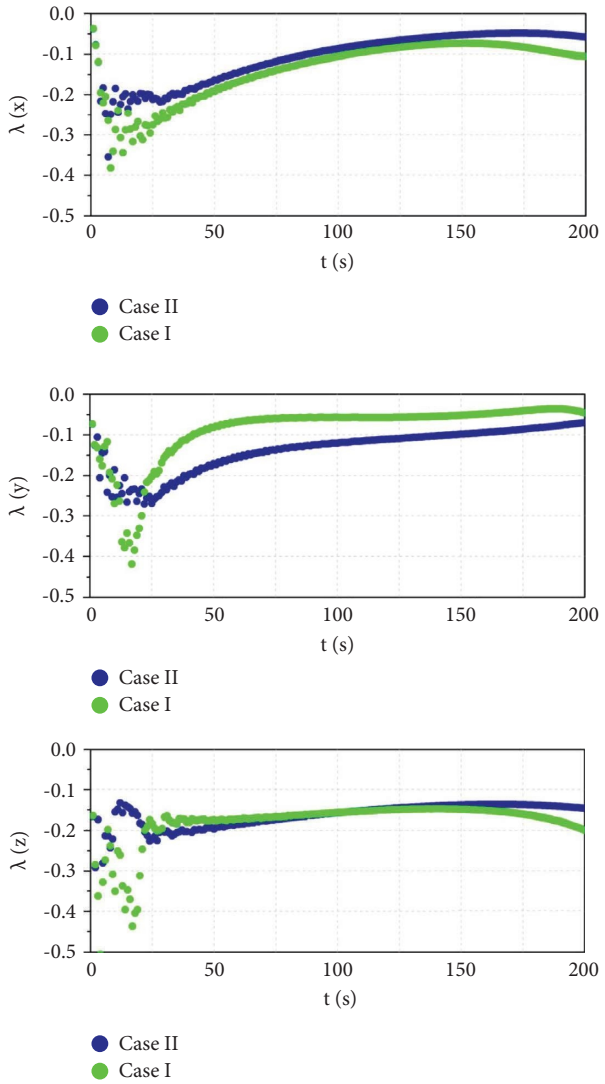


Figure 4: Lyapunov exponent spectrum.

be improved by changing the load mass. Within a certain range, the smaller the load mass, the better the motion stability of the system in the stationary hovering state.

*4.2. Optimization of Structure Features.* It is known from Figure 2, the mechanical feature $L$ has an impact on the Lyapunov exponent of the quadrotor. Next, the Lyapunov exponent of the attitude when the wheelbase $L$ changes is calculated, respectively. In the CASE 1, when the load mass and other features remain unchanged, only the wheelbase $L = 0.36$, $L = 0.55$, $L = 0.82$ are changed, and the simulation results are shown in Figures 5 and 6.

Figures 5 and 6: Changes in the mechanical structure can improve the motion stability of the quadrotor. It can be observed that when only the $L$ parameter is varied for the quadrotor, within a certain range, the larger the value of $L$, the faster the Lyapunov exponent of the system's attitude converges to zero, indicating better stability of the quadrotor in a stationary hovering state with a load. Therefore, by adjusting the $L$ parameter, the motion stability of the quadrotor in load hovering can be improved.

*4.3. Energy Consumption Optimization.* For the payload flight of a quadrotor, based on the above research, the influence of different system parameters on the total input energy spectrum was established using Mathematica software, as shown in Figure 7.

Figure 7:

(1) During the initial hovering phase of the quadrotor with load, i.e., $(0 \leqq t \leqq 10\text{s})$, the system is unstable due to airflow disturbances, resulting in an increase in energy consumption and the presence of an energy consumption peak.

(2) As the load mass decreases from 1.02 kg to 0.56 kg, the system's motion stability improves, and the energy consumption decreases correspondingly as the system does less work to overcome disturbances. By calculation, at t = 50s, the energy consumption in CASE 1 is 31.11% lower than in CASE 2.

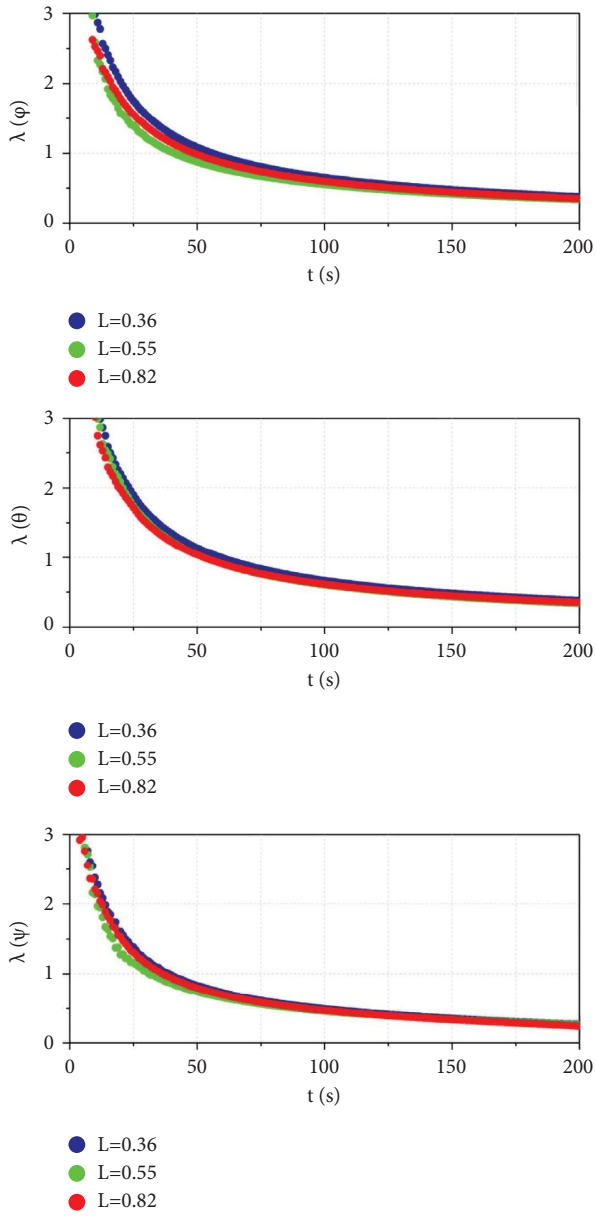


Figure 5: Lyapunov exponent spectrum.

(3) Through simulation analysis, the feasibility of using the Lyapunov exponent method to analyze system motion stability is verified, and it is shown that changing the structural parameters of the quadrotor can solve the issues of energy consumption and motion stability of the system.

## 5. Flight Experiment Testing and Analysis

The experimental platform uses Pixhawk as the flight control, a wheelbase $L = 0.36$, a fully enclosed four-axis rack, 2312A brush fewer motor, Hobbywing 20A ESC and 4S 5300 mAh battery. The quadrotor uses 3DR wireless data transmission module to realize communication with MP ground station, as shown in Figure 8.

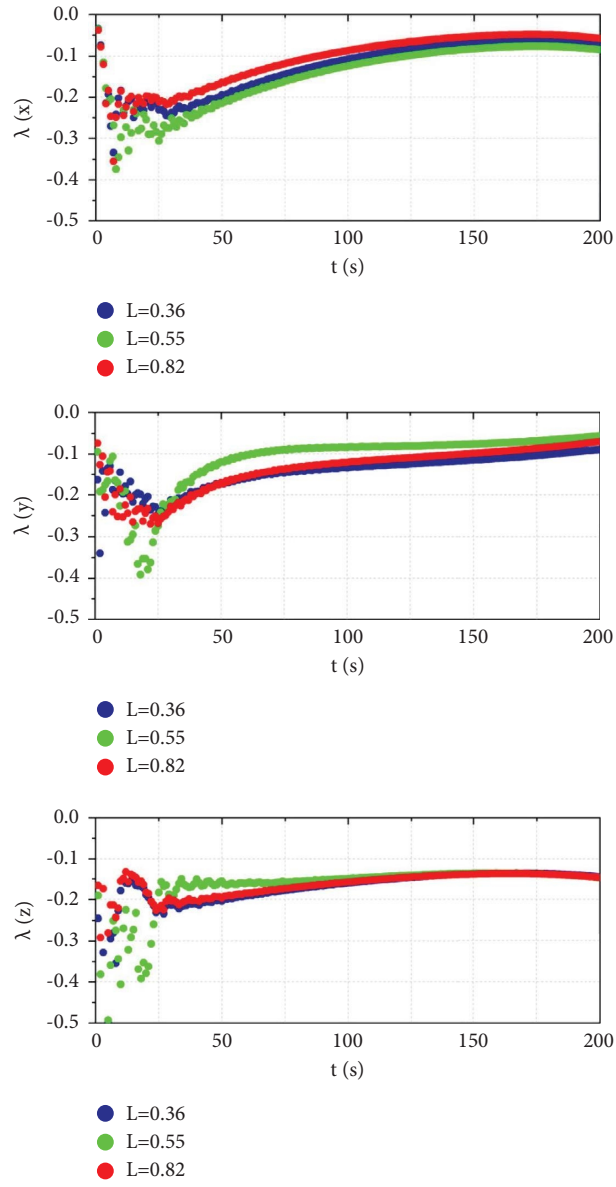


Figure 6: Lyapunov exponent spectrum.

*5.1. System Attitude Stability Test.* In the CASE 1, the optimization of different load features is used for experimental confirmation, and the flight attitude stability under position hovering state is analyzed.

Figure 9:

(1) Figure 9(a) shows the flight attitude information of the quadrotor with no load. It can be seen from the figure that there is no change in PITCH and YAW, and the error in ROLL angle is small, indicating good hovering stability.

(2) Figure 9(b) shows the flight attitude information of the quadrotor with a load of 0.56 kg. It can be seen from the figure that there is a relatively small change in PITCH and YAW, and the error in ROLL angle is between 25° and 40°, indicating relatively good hovering stability.

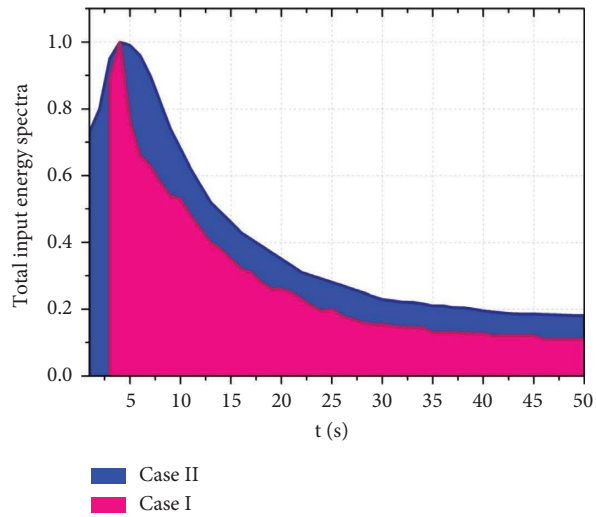


Figure 7: The influence of different features on the energy spectrum.

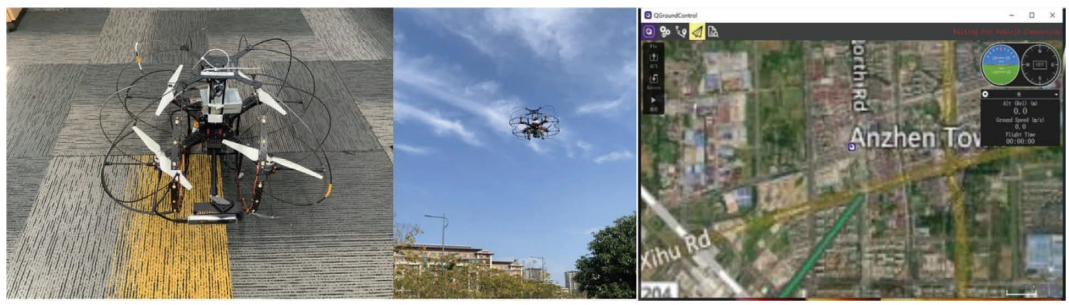


Figure 8: Quadrotor and ground station.

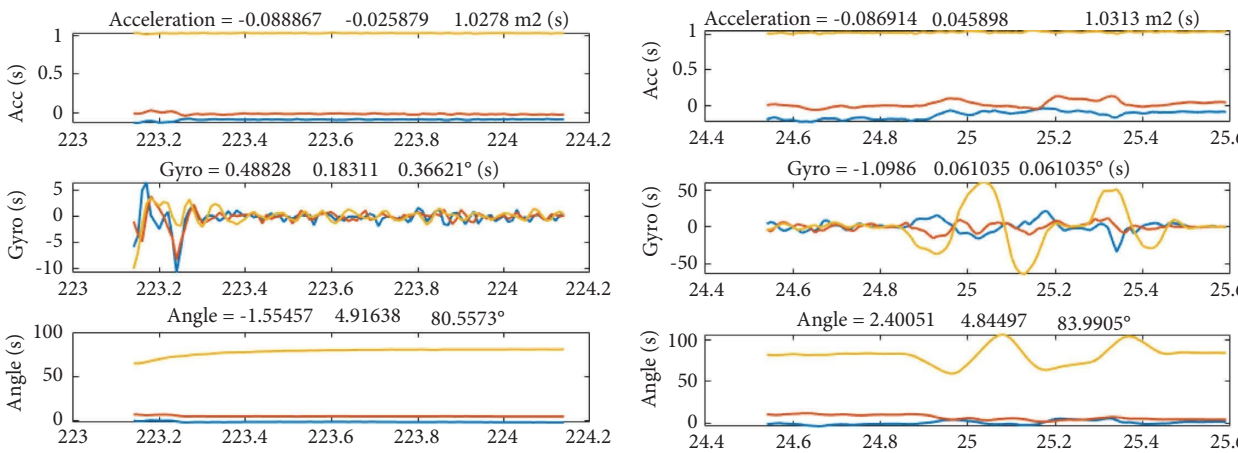


(a) (b)

Figure 9: Continued.

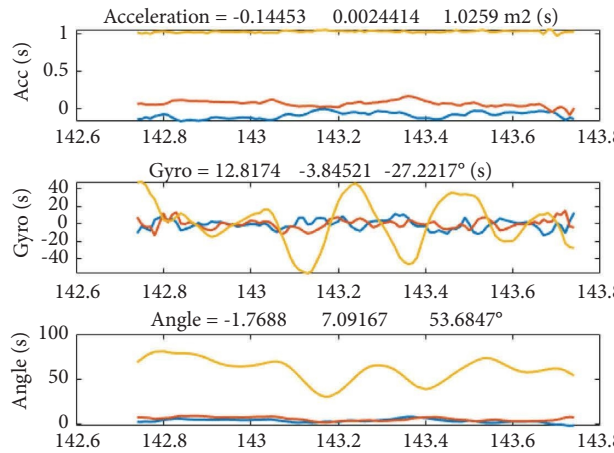


(c)

Figure 9: (a) No-load attitude curve, (b) $m = 0.56$ kg load attitude curve, and (c) $m = 1.02$ kg load attitude curve.

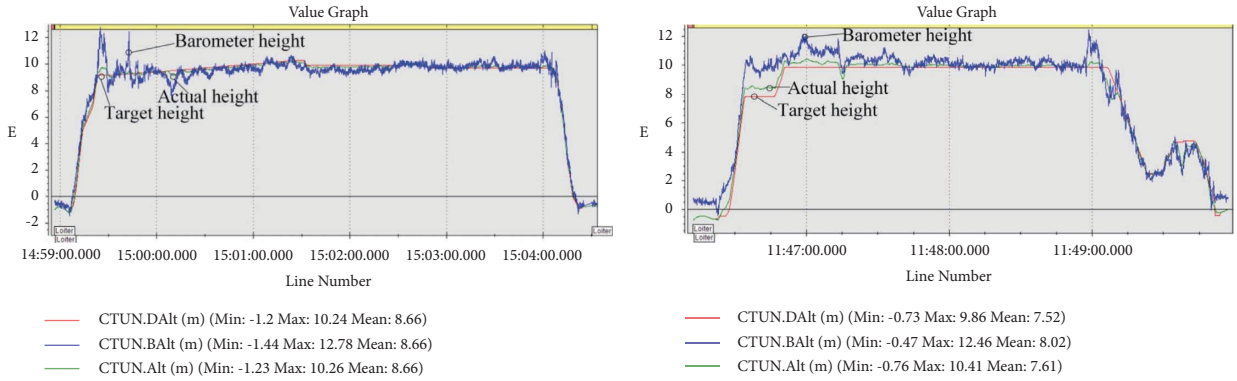


(a) (b)

Figure 10: (a) $M = 0.56$ kg load height curve. (b) $M = 1.02$ kg load height curve.

(3) Figure 9(c) shows the flight attitude information of the quadrotor with a load of 1.02 kg. It can be seen from the figure that there is a relatively small change in PITCH and YAW, but the error in ROLL angle is between 30° and 70°, indicating a large error in hovering angle.

In summary, the motion stability of the quadrotor can be improved within a certain payload range. When unloaded, the system structure parameters remain unchanged, resulting in the best stability for the quadrotor. The smaller the negative load, the smaller the attitude angle changes of the quadrotor, resulting in better payload flight stability.

*5.2. System High Stability Test.* In CASE 1, experimental verification was conducted using flight log data to analyze the stability of flight height during stationary hovering.

As shown in Figure 10 the observations are as follows:

(1) Figure 10(a) shows the flight height curve for a negative load of M = 0.56 kg. According to the requirements of the stationary flight mode, the target height coincides with the actual height, and the measured height by the barometer is basically consistent with the actual height, indicating good stability of the load flight.

(2) Figure 10(b) shows the flight height curve for a negative load of M = 1.02 kg. According to the requirements of the stationary flight mode, there is a deviation between the target height and the actual height, and the measured height by the barometer fluctuates significantly compared to the actual height. The stability of the load flight curve is worse than that of Figure 10(a).

As shown in Figure 11 the observations are as follows:

Under the stationary flight mode with a negative load of M = 1.02kg, at a flight height of h = 10m, the flight time $T_{max}$ = 11 (min) in minutes of the quadrotor is calculated based on battery life, given the load weight $G_{maxload}$ = 1.02kg of the quadrotor.

In summary, the maximum payload capacity is a fundamental performance indicator of the quadrotor and is closely related to safety. The smaller the payload, the less variation there will be in the height stability of the quadrotor, resulting in better load flight stability.

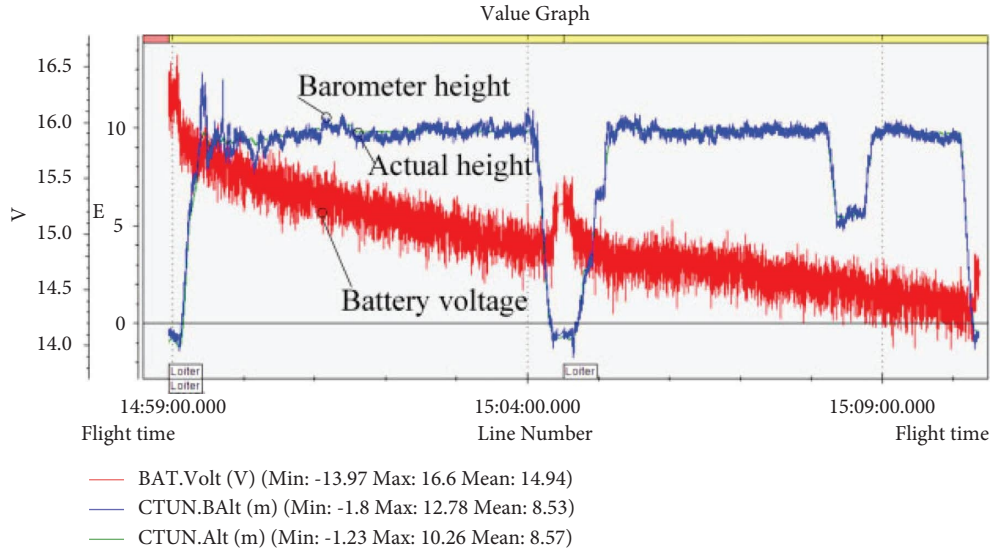


Figure 11: The endurance curve.

## 6. Experimental Results

This paper investigates the motion stability of a quadrotor during payload delivery using the Lyapunov exponent method based on the dynamic equations. The relationship between the payload parameters and the system's motion stability is quantitatively established, and the effects of changing structural and payload parameters on the quadrotor's stability are analyzed through simulation experiments. An experimental platform is also built to verify the impact of different loads on the stability of the quadrotor. The results obtained are as follows:

(1) The quantitative relationship between the payload mass, structural parameters, and the system's motion stability is elucidated, providing a theoretical basis for optimizing the control system. The experimental results show that within a certain range, smaller payload mass and a larger wheelbase result in better system stability.

(2) The relationship between the flight altitude experiment and the system's motion stability is also presented, which is significant for calculating the payload size. The experiment verifies that changes in payload mass directly affect the flight stability.

(3) The maximum payload weight is a fundamental performance indicator for quadrotor and is closely related to safety.

## Data Availability

The data used to support the findings of this study are available from the corresponding author upon request.

## Conflicts of Interest

The authors declare that they have no conflicts interests.

## Acknowledgments

This study was supported by the National Natural Science Foundation of China (grant no. 41875027), Jiangsu Province Modern Agricultural Machinery Equipment and Technology Demonstration and Promotion Project (grant no. NJ2022-02), and Jiangsu Province ASIC Key Laboratory Open Foundation (grant no. 2021KLOP005).

## References

[1] N. Suthanthira Vanitha, L. Manivannan, T. Meenakshi, and K. Radhika, "Stability analysis of quadrotor using state space mathematical modeling," *Materials Today: Proceedings*, vol. 33, no. 7, pp. 4040–4043, 2020.

[2] Y. H. Zhang, T. T. Dong, and Y. P. Liu, "Design of meteorological element detection platform for atmospheric boundary layer based on quadrotor," *International Journal of Aerospace Engineering*, vol. 14, Article ID 1831676, 2017.

[3] Z. J. Wang, L. Chen, and S. J. Guo, "Numerical analysis of aerodynamic characteristics for the design of a small ducted fan aircraft," *Proceedings of the Institution of Mechanical Engineers, Part G: Journal of Aerospace Engineering*, vol. 227, no. 10, pp. 1556–1570, 2013.

[4] C. Yang, J. Zhang, and Z. Huang, "Numerical study on cavitation-vortex-noise correlation mechanism and dynamic mode decomposition of a hydrofoil," *Physics of Fluids*, vol. 34, no. 12, Article ID 125105, 2022.

[5] M. E. Guerrero-Sánchez, O. Hernández-González, R. Lozano, C. D. García-Beltrán, G. Valencia-Palomo, and F. R. López-Estrada, "Energy-based control and LMI-based control for a quadrotor transporting a payload," *Mathematics*, vol. 7, no. 11, 2019.

[6] L. Liu, S. Zhang, L. Zhang, G. Pan, and J. Yu, "Multi-UUV maneuvering counter-game for dynamic target scenario based on fractional-order recurrent neural network," *IEEE Transactions on Cybernetics*, pp. 1–14, 2022.

[7] M. E. Guerrero-Sánchez, R. Lozano, P. Castillo, O. Hernández-González, C. García-Beltrán, and G. Valencia-Palomo, "Nonlinear control strategies for a UAV carrying

a load with swing attenuation," *Applied Mathematical Modelling*, vol. 91, pp. 709–722, 2021.

[8] X. Q. Zeng, Y. G. Zou, Z. X. Zhou et al., "On the deflection of composite reinforced steel truss-concrete beam under static and dynamic load," *Journal of Computational Methods in Science and Engineering*, vol. 22, no. 5, pp. 1533–1544, 2022.

[9] O. Köse and T. Oktay, "Combined quadrotor autopilot system and differential morphing system design," *Journal of Aviation*, vol. 5, no. 2, pp. 64–71, 2021.

[10] N. Amiri, A. Ramirez-Serrano, and R. J. Davies, "Integral backstepping control of an unconventional dual-fan unmanned aerial vehicle," *Journal of Intelligent and Robotic Systems*, vol. 69, no. 1-4, pp. 147–159, 2013.

[11] Y. P. Liu, X. Y. Li, T. M. Wang, Y. H. Zhang, and P. Mei, "Quantitative stability of quadrotor unmanned aerial vehicles," *Nonlinear Dynamics*, vol. 87, no. 3, pp. 1819–1833, 2017.

[12] Y. Hu, J. X. Qing, Z. H. Liu, Z. J. Conrad, J. N. Cao, and X. P. Zhang, "Hovering efficiency optimization of the ducted propeller with weight penalty taken into account," *Aerospace Science and Technology*, vol. 117, Article ID 106937, 2021.

[13] G. Zhou, X. Bao, S. Ye, H. Wang, and H. Yan, "Selection of optimal building facade texture images from UAV-based multiple oblique image flows," *IEEE Transactions on Geoscience and Remote Sensing*, vol. 59, no. 2, pp. 1534–1552, 2021.

[14] C. Chen, T. T. Dong, W. J. Fu, and N. Liu, "On dynamic characteristics and stability analysis of the ducted fan unmanned aerial vehicles," *International Journal of Advanced Robotic Systems*, vol. 16, no. 4, Article ID 172988141986701, 2019.

[15] C. X. Yang and C. Q. Wu, "A robust method on estimation of Lyapunov exponents from a noisy time series," *Nonlinear Dynamics*, vol. 64, no. 3, pp. 279–292, 2011.

[16] C. Chen, L. R. Zhang, C. Zhang, W. J. Fu, and N. Liu, "Stability analysis and structural features optimization of quadrotor unmanned aerial vehicles," *International Journal of Plant Engineering and Management*, vol. 24, no. 1, pp. 19–29, 2019.

[17] Y. P. Liu, C. Chen, H. T. Wu, Y. H. Zhang, and P. Mei, "Structural stability analysis and optimization of the quadrotor unmanned aerial vehicles via the concept of Lyapunov exponents," *The International Journal of Advanced Manufacturing Technology*, vol. 94, no. 9-12, pp. 3217–3227, 2018.

[18] J. Awrejcewicz and G. Kudra, "Stability analysis and Lyapunov exponents of a multi-body mechanical system with rigid unilateral constraints," *Nonlinear Analysis: Theory, Methods and Applications*, vol. 63, no. 5-7, pp. e909–e918, 2005.

[19] S. Sadri and C. Q. Wu, "Modified Lyapunov exponent, new measure of dynamics," *Nonlinear Dynamics*, vol. 78, no. 4, pp. 2731–2750, 2014.

[20] C. X. Yang and Q. Wu, "On stability analysis via Lyapunov exponents calculated from a time series using nonlinear mapping—a case study," *Nonlinear Dynamics*, vol. 59, no. 1-2, pp. 239–257, 2010.

[21] Y. M. Sun and C. Q. Wu, "Stability analysis via the concept of Lyapunov exponents—a case study in optimal controlledbiped standing," *International Journal of Control*, vol. 85, no. 12, pp. 1952–1966, 2012.

[22] M. Polajnar, F. Kosel, and R. Drazumeric, "Structural optimization using global stress-deviation objective function via the level-set method," *Structural and Multidisciplinary Optimization*, vol. 55, no. 1, pp. 91–104, 2017.

[23] Y. Gao, "New energy vehicle engine speed control method based on vehicle networking technology," *Journal of Computational Methods in Science and Engineering*, vol. 22, no. 6, pp. 2201–2215, 2022.

[24] A. J. McCall and R. J. Balling, "Structural analysis and optimization of tall buildings connected with skybridges and atria," *Structural and Multidisciplinary Optimization*, vol. 55, no. 2, pp. 583–600, 2017.

[25] Y. P. Liu, X. Y. Li, T. M. Wang, Y. H. Zhang, and P. Mei, "Quantitative stability of quadrotor unmanned aerial vechicle during yawing," *Nanjing Li Gong Daxue Xuebao/Journal of Nanjing University of Science and Technology*, vol. 40, no. 5, pp. 520–526, 2016.